Strained silicon: A dielectric-response calculation

Zachary H. Levine, Hua Zhong, and Siqing Wei*
Department of Physics, The Ohio State University, Columbus, Ohio 43210-1106

Douglas C. Allan
Applied Process Research, SP-PR-22, Corning Incorporated, Corning, New York 14831
and Department of Physics, The Ohio State University, Columbus, Ohio 43210-1106

John W. Wilkins
Department of Physics, The Ohio State University, Columbus, Ohio 43210-1106
(Received 14 August 1991)

Strain-induced birefringence is calculated with crystalline silicon for pressure applied along the [001] and [111] directions of the crystal. Results for the dielectric function and its change under hydrostatic strain are also given. The results are calculated for photon energies in the range 0–3.25 eV, i.e., below the direct band gap. We have made a fully-self-consistent Kohn-Sham local-density-approximation calculation, in the pseudopotential, plane-wave scheme, with a self-energy correction in the form of a rigid shift of the conduction bands of magnitude $\Delta=0.9$ eV. Agreement with experiment is very good in the static limit, considering disagreements among the experimental values. Values of the photoelastic tensor for [001] strain are $p_{11}-p_{12}=-0.118$ (theory) and -0.111 ± 0.005, -0.127 ± 0.005 (expt.). For [111] strain, we obtain $p_{44}=-0.050$ (theory) and -0.051 ± 0.002, -0.051 ± 0.002 [sic] (expt.); for hydrostatic distortions, $p_{11}+2p_{12}=-0.067$ (theory) and -0.055 ± 0.006, -0.070 ± 0.008 (expt.). For the static dielectric constant, we obtain 10.9, compared to 11.7 and 11.4 (0 K) (expt.). All experiments quoted are at room temperature, except as noted. Above 2 eV, the calculation predicts less dispersion than seen by the experiments. Thermal effects and electron-hole interactions are estimated to resolve some of the discrepancies with experiment. The experimental data for [001] strains is not consistent with a single-oscillator model, and is therefore suspect.

I. INTRODUCTION

When a cubic crystal is strained, the normally isotropic dielectric tensor becomes anisotropic. For small distortions, the linear relationship between the change in the inverse dielectric function and the strains form the photoelastic tensor. At least two groups have measured these coefficients for strained silicon. Biegelsen has measured the photoelastic coefficients for frequencies below the indirect band gap.[1] Cardona and co-workers performed a similar measurement[2] and subsequently extended their work to frequencies between the indirect and direct band gaps.[3,4] On the whole, these measurements are in agreement. For the case of isotropic strain, the agreement among the experiments is somewhat less satisfactory, as reviewed in Ref. 5.

Semiempirical models of the optical properties of strained silicon have been reviewed,[1] but there has never been a calculation using "first-principles" techniques to our knowledge in silicon, or any other material; however, a sophisticated calculation of the band gap in diamond under [001] stress has been performed recently.[6] The purpose of the present paper is to present a calculation of silicon under arbitrary anisotropic strains. In the past, two of us have studied other optical properties of solids, specifically the dielectric function of semiconductors[5,7–9] and the nonlinear susceptibility for second-harmonic generation.[8,9] Our approach (in both these works and the present) is as follows: first, we perform a well-converged Kohn-Sham local-density-approximation (LDA) calculation using plane waves and pseudopotentials to obtain a ground-state potential.[10] Second, in calculating optical response, we use a modified Hamiltonian

$$H_{\mathbf{k}}=H_{\mathbf{k}}^{\mathrm{LDA}}+\Delta_{\mathbf{k}}P_{c\mathbf{k}}\ , \tag{1}$$

where $H_{\mathbf{k}}^{\mathrm{LDA}}$ is the LDA Hamiltonian at a point $\mathbf{k}$ in the Brillouin zone, $\Delta_{\mathbf{k}}$ is an energy shift, and $P_{c\mathbf{k}}$ is the projection operator onto the conduction bands at $\mathbf{k}$. The term $\Delta_{\mathbf{k}}P_{c\mathbf{k}}$ is sometimes called a "scissors" operator. This energy shift represents a self-energy correction that may be obtained through a many-body calculation in the GW approximation.[11–14] In practice, we do not include the k dependence of the self-energy correction, which is on the order of 0.1 eV for silicon.[13] Generally, the self-energy-corrected LDA has been quite successful in predicting optical properties of semiconductors, leading, e.g., to disagreement with experimental value of the static limit of the dielectric function ϵ_∞ of a few percent for some six cases.[5,7–9] Our interest in strained silicon arises from the desire to test the range of applicability of this approximation. Ultimately, our goal is the reliable prediction of optical properties of semiconductors that have not even been fabricated. Some of the problems we address in strained silicon will arise later in studies of

strained-semiconductor heterostructures.

Our theory has been presented extensively recently,[5] so it is omitted here. (However, we opted for finding virtual levels through direct diagonalization as in Refs. 8 and 9 rather than the iterative solution of the inhomogeneous Schrödinger equation.) Briefly, we are solving for the dielectric function with local-field corrections using the scheme presented by Adler[15] and Wiser,[16] using the LDA Hamiltonian modified by a self-energy correction in the form of a scissors operator, as shown in Eq. (1).

II. SYMMETRY CONSIDERATIONS

A cubic crystal is optically isotropic. When the crystal is strained anisotropically, its symmetry is lowered, and the crystal becomes birefringent. For a general strain, the resulting dielectric tensor has three independent components, i.e., it is biaxial. Certain particular strains render the crystal optically uniaxial. Compression in the [001] direction changes the crystal class from cubic to tetragonal; for compression in the [111] direction, it becomes trigonal. Both the tetragonal and trigonal crystal classes are optically uniaxial; the directions are fixed by the crystal geometry and are independent of the frequency of light passing through them.[17]

The change in the dielectric tensor due to strain is often described by the photoelastic tensor p_{ijkl},

$$\delta(1/\epsilon_{ij})=p_{ijkl}\mu_{kl} \ , \tag{2}$$

where the strain is given by the μ_{kl}; we use the Einstein-summation convention in this paper. The strain is symmetric in its two indices; in the absence of magnetic fields or absorption, the dielectric tensor (and its inverse) are also symmetric. The tensor p_{ijkl} is a fourth-rank tensor that is symmetric in both pairs of symmetric indices. We use a compressed notation for such a tensor. Specifically, the index pairs are mapped: $11\rightarrow1$, $22\rightarrow2$, $33\rightarrow3$, $23,32\rightarrow4$, $13,31\rightarrow5$, and $12,21\rightarrow6$. We refer to the resulting set of six values as a "six-vector"; these index pairs may be used for vector and matrix multiplications, but do not have the coordinate-transformation properties of a vector. We adopt the conventions of Grimsditch *et al.*,[4] $p_{\alpha\beta}=p_{ijkl}$, where ij and kl correspond to α and β, respectively, with similar relations for σ, $\delta(1/\epsilon)$, and c, but for π and μ relations such as ($\pi_{ijkl}=\pi_{\alpha\beta}$, $\alpha,\beta=1,2,3$) and ($2\pi_{ijkl}=\pi_{\alpha\beta}$, $\alpha,\beta=4,5,6$) hold. The variables σ, c, and π represent the stress, elastic-moduli, and piezobirefringence tensors, respectively. For silicon's point group, O_h, such a tensor will have three independent components. The tensor takes the form[18]

$$p=\begin{vmatrix} p_{11} & p_{12} & p_{12} & 0 & 0 & 0 \\ p_{12} & p_{11} & p_{12} & 0 & 0 & 0 \\ p_{12} & p_{12} & p_{11} & 0 & 0 & 0 \\ 0 & 0 & 0 & p_{44} & 0 & 0 \\ 0 & 0 & 0 & 0 & p_{44} & 0 \\ 0 & 0 & 0 & 0 & 0 & p_{44} \end{vmatrix} . \tag{3}$$

This matrix may be diagonalized. The eigenvalues (and degeneracies) are $p_{11}+2p_{12}$ (1), $p_{11}-p_{12}$ (2), and p_{44} (3). The eigenvector, i.e., the strain, corresponding to the first eigenvector is a uniform compression. The eigenvectors of strain for the second eigenvalue may be chosen to be a compression along one Cartesian axis with a volume-conserving expansion in the other two directions. For the third eigenvalue, the eigenvectors may be viewed as a contraction in a bonding direction with a volume-conserving expansion in the orthogonal plane.

The piezobirefringence tensor π relates the changes in the inverse dielectric function to stresses σ_{kl} via

$$\delta(1/\epsilon_{ij})=\pi_{ijkl}\sigma_{kl} \ . \tag{4}$$

Experimentally, a stress is placed along the [001], [111], or [110] direction, or applied hydrostatically, leading to a measurement of certain linear combinations of components of the piezobirefringence tensor. In our calculation, we model a strain in the [001] or [111] direction, or a hydrostatic distortion. The elastic moduli, defined by the relation

$$\sigma_{kl}=c_{ijkl}\mu_{ij} \ , \tag{5}$$

may be used to relate the photoelastic tensor to the piezobirefringence tensor:

$$p_{ijkl}=\pi_{ijmn}c_{mnkl} \ . \tag{6}$$

The tensors π and c have the same symmetry as p given in Eq. (3). In practice, comparison to experiment is facilitated because we are only concerned with those linear combinations of the tensor coefficients which are eigenvalues. Since, viewed as matrices, these are simultaneously diagonalizable, conversion from π to p involves a single scalar multiplication. Explicitly,

$$\begin{aligned} p_{1111}+2p_{1122}&=(\pi_{1111}+2\pi_{1122})(c_{1111}+2c_{1122}) \ , \\ p_{1111}-p_{1122}&=(\pi_{1111}-\pi_{1122})(c_{1111}-c_{1122}) \ , \end{aligned} \tag{7}$$

and

$$p_{1212}=\pi_{1212}c_{1212} \ .$$

The strains we consider are uniform compression; compression of the [001] direction only, leaving the other directions fixed; and compression of the [111] direction only, leaving the other directions fixed. (Our [001] and [111] compressions are not eigenvectors of the matrix p in Eq. (3) since they result in a change in volume.) From uniform compression, we determine the linear combination $p_{11}+2p_{12}$. From the [001] compression, we determine both p_{11} and p_{12}, and hence $p_{11}-p_{12}$ and $p_{11}+2p_{12}$. From [111] compression, we find p_{44} and $p_{11}+2p_{12}$. The three ways of determining $p_{11}+2p_{12}$ represent an internal consistency check, as discussed below.

To determine these photoelastic constants, we calculate the dielectric functions under different strains. Under hydrostatic strain,

$$[\mu]=\frac{\delta a}{a}(1,1,1,0,0,0)^T \ , \tag{8}$$

where δa is the change in lattice constant and the super-

script T is the transpose symbol. The symbol "[$\cdots$]" denotes a "six-vector." Using the definition of the photoelastic constant,

$$\delta[1/\epsilon]=[p][\mu] = \frac{\delta a}{a}(p_{11}+2p_{12}, p_{11}+2p_{12}, p_{11}+2p_{12}, 0, 0, 0)^T , \tag{9}$$

$p_{11}+2p_{12}$ can be determined from the difference between the strained and unstrained dielectric constant $\delta[1/\epsilon]$, using

$$\delta[1/\epsilon]=\frac{\delta a}{a}\begin{bmatrix} p_{11}+2p_{12} & 0 & 0 \\ 0 & p_{11}+2p_{12} & 0 \\ 0 & 0 & p_{11}+2p_{12} \end{bmatrix} . \tag{10}$$

Under a strain in [001] direction,

$$[\mu]=\frac{\delta a}{a}(0,0,1,0,0,0)^T , \tag{11}$$

the difference of the dielectric matrix becomes

$$\delta[1/\epsilon]=\frac{\delta a}{a}\begin{bmatrix} p_{12} & 0 & 0 \\ 0 & p_{12} & 0 \\ 0 & 0 & p_{11} \end{bmatrix} . \tag{12}$$

The other element in the photoelastic matrix p_{44} can be determined by changing the length in the [111] direction by δl, i.e., by the strain

$$[\mu]=\frac{1}{3}\frac{\delta l}{l}(1,1,1,2,2,2)^T . \tag{13}$$

The factor 2 involved in the formula comes from the definition stated above. Again, from the definition of the photoelastic constant,

$$\delta[1/\epsilon]=\frac{1}{3}\frac{\delta l}{l}\begin{bmatrix} p_{11}+2p_{12} & 2p_{44} & 2p_{44} \\ 2p_{44} & p_{11}+2p_{12} & 2p_{44} \\ 2p_{44} & 2p_{44} & p_{11}+2p_{12} \end{bmatrix} . \tag{14}$$

The [111] strain permits an internal degree of freedom, often denoted by ζ. Under a [111] strain, the bond length between two silicon atoms joined in the [111] direction may vary, but the direction will be unchanged. As indicated in Table I, $\zeta=0$ indicates the atoms connected along [111] are shifted uniformly with the strain, and $\zeta=1$ indicates this pair of atoms retains its unstressed bond length. These two points suffice to define a scale for the final bond position, but we refer the reader elsewhere for a mathematical definition.[19–22]

III. RESULTS

We have calculated the various independent components of the photoelastic tensor using the method described in the preceding sections. Our default parameters are given in Table II; that is, these conditions are used except when we explicitly state they are varied in a sensitivity test. Compared to a previous study by some of us,[5] we have increased the plane-wave energy cutoff from 9 hartrees to 10 hartrees, used the experimental lattice constant at 300 K rather than 0 K, and corrected a small, previously reported programming error[9] which shifts the calculated dielectric function by about -2% upon correction.

Our results for silicon under hydrostatic strain are plotted in Fig. 1. There have been a number of measurements of this quantity, as collected by Ref. 5, for example; here we only present two that we believe to be authoritative. Their static limits are almost in agreement with each other: for $p_{11}+2p_{12}$, Biegelsen gives a value of -0.055 ± 0.006 compared to Vetter's -0.070 ± 0.008. The present study predicts -0.062, which is in marginal agreement with the both values. The calculated frequency dependence is a reasonable description of the experimental data. We are not aware of data in the region above the indirect band gap, so the test of frequency dependence is not particularly stringent in this case.

In Fig. 2 the calculated photoelastic-tensor component $p_{11}-p_{12}$ is given for strain in the [001] direction. Below the indirect band gap, our calculated values are between the two data sets. While this indicates our theory is reasonable, it gives no support for either set of measure-

TABLE I. Characteristics of special values of the parameter ζ, which describes the bond length along the [111] direction under strain in the [111] direction. For the unstressed system, the bond lengths along [111], [$\bar{1}$11], [1$\bar{1}$1], and [11$\bar{1}$] are all equal, but with stress along [111] there are two distinct values for the bond lengths: [111] and the others. Similarly, in the unstressed case, there is one value for the bond angle, but under [111] strain there are two distinct values for the bond angles. (When the phrase "under compression" appears, under expansion the sign of the indicated phenomenon is reversed.)

ζ	Remark
$-\frac{1}{3}$	all bond angles equal
$>-\frac{1}{3}$	[111][$\bar{1}$11] angle less than [$\bar{1}$11][1$\bar{1}$1] angle under compression
0	change in [111] is proportional to overall change in [111] direction
$<\frac{2}{3}$	[111] bond shorter than other bonds under compression
$\frac{2}{3}$	all bond lengths equal
$>\frac{2}{3}$	[111] bond longer than other bonds under compression
1	modified [111] bond length equals uncompressed [111] bond length

TABLE II. Default parameters for calculation in this paper. Only the changes from these values will be noted in the other tables and the figures. The "equivalent number of **k** points" refers to the number of integration points [or "special points" (Ref. 23)] in the irreducible Brillouin zone of the diamond structure; see Table VII for more information. Photoelastic-tensor components were found using the indicated finite-difference scheme.

Plane-wave energy cutoff	10 hartrees
Self-energy correction Δ	0.9 eV
Equivalent number of **k** points	60
Lattice constant	10.2646 bohr (300-K expt.)
Bands retained	hydrostatic, 250; [001], 100; [111], 70
Finite differences	at lattice constants of $\pm 1\%$ of nominal
Pseudopotential	Hamann,[a] separable[b]
Exchange-correlation potential	Ceperley and Alder,[c] Teter[d]
Core corrections	none

[a]Reference 31.
[b]Reference 32.
[c]Reference 33.
[d]Reference 34.

ments over the other. Above the indirect band gap, our calculated dispersion is less than half that of the experiment. As discussed below, this may be due to a combination of thermal effects, particle-hole interactions, and errors in the experiments beyond the reported uncertainties.

The third independent component of the photoelastic tensor p_{44} is given for stress in the [111] direction. As discussed in Sec. II and Table I, the variable ζ is a measure of the relaxation of the [111] bond under stress. The value $\zeta=0.53$ is predicted by two independent LDA total-energy calculations;[21,22] and a semiempirical model.[22] The value $\zeta=0.53$ is made plausible by noting that $\zeta=\frac{2}{3}$ if the bond energy were totally determined by bond lengths alone, and $\zeta=-\frac{1}{3}$ if determined by bond-angle energies alone. The value suggested by the LDA calculations is about $\frac{1}{7}$ of the way from the "bond-length-only" value to the "bond-angle-only" value, indicating bond lengths dominate the energetics, but bond angles play a significant role.

Both measurements[1,2] of p_{44} happen to have the identical value of -0.051 ± 0.002, which is in agreement with our calculated value of -0.050. As seen in Fig. 3, our calculation gives an excellent account of the low-frequency behavior, but does less well with the dispersion. Although particle-hole interactions and thermal effects may account for this problem, as we proposed for the [001] strain, we have no evidence that this is the case. At first glance, it appears that a smaller value of ζ might fit the data, but it does not appear possible to obtain good agreement above the band gap without destroying the already good agreement in the static limit. Figure 4 illustrates that p_{44} is approximately a linear function of ζ in the frequency range of interest.

There may be problems with the measurement. Reference 4 was a refinement of Ref. 3. The remeasurement allowed them to take into account effects of optical absorption above the band gap on their reported values because of an inconsistency between the earlier measurements

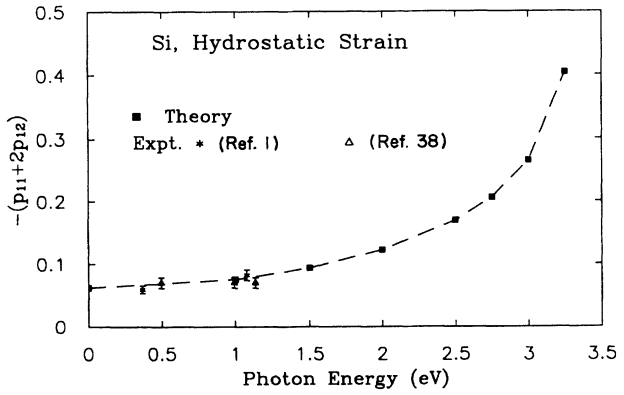

FIG. 1. Photoelastic coefficient $p_{11}+2p_{12}$ as a function of photon energy for silicon under hydrostatic strain, compared to experimental data from Biegelsen (Ref. 1) and Vetter (Ref. 38).

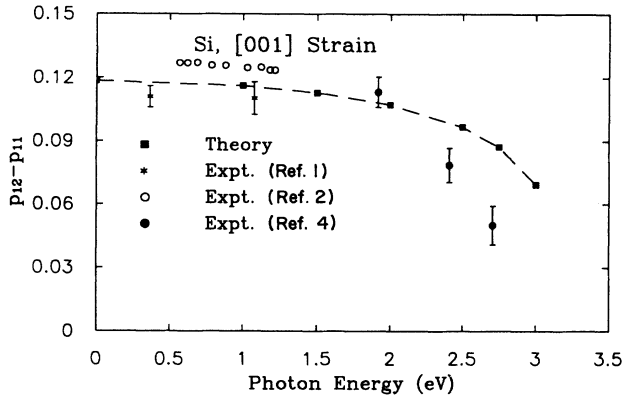

FIG. 2. Photoelastic coefficient $p_{12}-p_{11}$ as a function of photon energy for silicon under a strain in the [001] direction. Experimental data are from Biegelsen (Ref. 1) and from Cardona and co-workers below (Ref. 2) and above (Ref. 4) the indirect band gap. As discussed in the text, by our estimate, thermal effects and electron-hole interactions should account for some of the difference between our calculation and experiment at the higher frequencies, but cannot reproduce the dispersion.

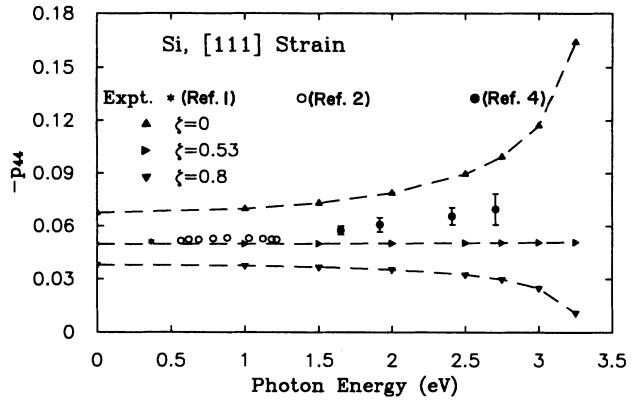

FIG. 3. Photoelastic coefficient p_{44} as a function of photon energy for silicon under a strain in the [111] direction. Sources for the experimental data are the same as in Fig. 2. The internal relaxation parameter ζ is defined in Sec. II and described in Table I. $\zeta=0.53$ is predicted by LDA total-energy calculations (Refs. 21 and 22); $\zeta=0$ is the value without internal relaxation of the [111] bond; $\zeta=0.8$ is an arbitrary third value. As discussed in the text, by our estimate, thermal effects and electron-hole interactions apparently will not account for the difference between our calculation and the experiment at higher frequencies.

(Ref. 3) and certain Raman-scattering data. Reference 4 gave a downward revision of the magnitude of p_{44} that was about twice the earlier error estimate, and the revised error estimate was increased by about $\frac{1}{3}$. Nevertheless, these authors concluded that even the revised values were not consistent with the Raman-scattering data.

We may gain a qualitative understanding of the behavior of the piezobirefringence coefficients. Imagine a two-level model, with an occupied bonding orbital and an unoccupied antibonding orbital. If the bond length is shortened, the energy splitting of the two levels will increase, and hence the polarizability in the direction of the bond will decrease. Perpendicular to the bond there will be little effect: our calculation indicates that the magnitude of the shift in dielectric function for the component parallel to the strain direction is some 6 times larger for the [001] strain and 16 times larger for the [111] strain than for the perpendicular component. These simple ideas also account for the ζ dependence of the coefficient p_{44}. The [111] bond-length change is less for larger ζ (up to 1). To the extent that the [111] bond dominates the changes in the polarizability, a larger value of ζ implies less change in the polarizability, and, hence, a smaller p_{44} than the result given by the purely kinematic distortion, $\zeta=0$. For hydrostatic compression, one expects, and finds, a decrease in polarizability with decreased lattice constant. However, at large pressures, silicon becomes metallic, so this simple picture necessarily breaks down.

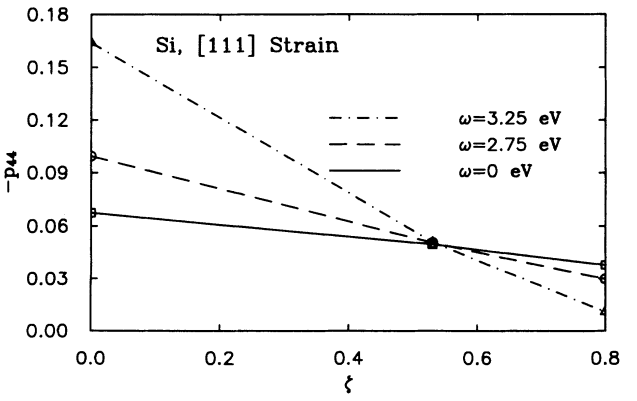

FIG. 4. Photoelastic coefficient p_{44} as a function of the internal shift ζ for three photon energies. p_{44} is seen to be roughly linear in ζ at all frequencies.

TABLE III. The photoelastic coefficient of hydrostatic strain, $p_{11}+2p_{12}$, calculated from various strains. (See Sec. II for a discussion of how these values are obtained.) The variable ζ only applies to [111] strain, with $\zeta=0.53$ being our estimate of the experimental value. Agreement at the 2% level is achieved between all cases, except [111] strain with $\zeta=0$.

	ζ	Photon energy (eV) 0	2.75	3.25
Hydrostatic strain		−0.062	−0.206	−0.404
[001] strain		−0.061	−0.203	−0.401
[111] strain	0	−0.236	−0.294	−0.432
	0.53	−0.063	−0.208	−0.410
	0.80	−0.063	−0.208	−0.402

A. Sensitivities

We noted in Sec. II that the photoelastic coefficient associated with hydrostatic strain, $p_{11}+2p_{12}$, may be calculated by applying a hydrostatic strain, a [001] strain, or a [111] strain. In principle, these values should be equal. We calculated $p_{11}+2p_{12}$ using the three different distortions; in the case of the [111] strain, we used three values of ζ. As seen in Table III, we find the various methods yield agreement at three photon energies within 2%, except for the unphysical case of $\zeta=0$. (Why $\zeta=0.80$, which is also unphysical, remains well behaved remains a

TABLE IV. The effect of lattice constant on the dielectric function and photoelastic tensor at three photon energies. The LDA lattice constant, obtained by minimizing the total energy in the LDA, is $a_{\mathrm{LDA}}=10.1733$ bohrs. The experimental lattice constant is $a_{\mathrm{expt}}=10.2646$ bohrs. As the band gap is approached, the sensitivity to lattice constant increases; see, in particular, $p_{11}-p_{12}$.

		Photon energy (eV) 0	2.75	3.25
ϵ	a_{LDA}	10.88	16.26	21.66
	a_{expt}	10.94	16.71	23.17
$p_{11}+2p_{12}$	a_{LDA}	−0.041	−0.165	−0.279
	a_{expt}	−0.062	−0.206	−0.404
$p_{11}-p_{12}$	a_{LDA}	−0.1193	−0.098	−0.067
	a_{expt}	−0.1184	−0.087	−0.017
p_{44}	a_{LDA}	−0.045	−0.045	−0.045
	a_{expt}	−0.050	−0.051	−0.051

TABLE V. The effect of the self-energy parameter Δ on the dielectric function and photoelastic tensor at two photon energies. As the band gap is approached, the sensitivity to Δ increases. The omitted values are too singular to be evaluated accurately in our integration scheme; $\omega=3.25$ eV and $\Delta=0.7$ eV also leads to unreliable values. $\Delta=0$ is the LDA.

		Photon energy (eV)	
	Δ	0	2.75
ϵ	0	13.2	
	0.7	11.4	18.6
	0.9	10.9	16.7
$p_{11}+2p_{12}$	0	−0.085	
	0.7	−0.067	−0.249
	0.9	−0.062	−0.206
$p_{11}-p_{12}$	0	−0.105	
	0.7	−0.115	−0.073
	0.9	−0.118	−0.087
p_{44}	0	−0.0459	
	0.7	−0.0489	−0.0500
	0.9	−0.0497	−0.0506

minor mystery.) This numerical agreement provides a limit on our overall accuracy, and is a verification of our code.

The *sensitivity to the lattice constant* of the calculation is studied in Table IV. For ϵ, $p_{11}-p_{12}$, and p_{44} the lattice-constant dependence is moderate, but, for $p_{11}+2p_{12}$, the lattice-constant dependence is quite large, varying by up to 50% for a change of less than 1% in the lattice constant. Typically, properties become very sensitive just below the direct band gap, which occurs at 3.58 eV in our calculation. In Table IV this enhanced sensitivity occurs for ϵ and $p_{11}-p_{12}$ for the 3.25-eV photon energy; indeed, the $p_{11}-p_{12}$ value is so sensitive that we feel it is unreliable. It is unfortunate that the property $p_{11}+2p_{12}$ is so sensitive to the lattice constant—for a novel material, the geometry would not be known in advance; if the LDA total-energy method is used to determine the geometries, this might be the largest source of error in the calculation. A similar issue arose in the case of the nonlinear susceptibility for second-harmonic generation.[8,9]

TABLE VI. Direct band gap of silicon for various conditions. The direct band gap occurs at Γ.

Source	Condition	Direct band gap
Present work	LDA	2.68 eV
Present work	$\Delta=0.7$ eV	3.38 eV
Present work	$\Delta=0.9$ eV	3.58 eV
Expt.[a]	300 K	3.45 eV
Expt.[b]	0 K	3.35 eV
Expt.[c]	4 K	3.4 eV
Expt.[c]	shift, 4–190 K	−50 meV

[a]Reference 35.
[b]Reference 36.
[c]Reference 37.

The *sensitivity to changes in self-energy correction* Δ is given in Table V. On *a priori* grounds we prefer the value of $\Delta=0.9$ eV, indicated by the *GW* calculation of Zhu and co-workers[14] that used a 9-hartree plane-wave energy cutoff, to $\Delta=0.7$ eV, which is suggested by two earlier *GW* calculations that employed energy cutoffs of 6.25 hartrees (Ref. 13) and 6.5 hartrees.[12] As illustrated in Table VI, $\Delta=0.7$ eV happens to make our eigenvalue-difference estimate of the direct band gap nearly equal to the experimental value. So we chose $\Delta=0.7$ eV as a reasonable comparison value; some LDA results, i.e., $\Delta=0$, are also given. As illustrated in Table V, in the static limit an adjustment of Δ by 0.2 eV has a rather modest effect (less then 10%) on the photoelastic-tensor components and ϵ. Near the direct band gap, the sensitivity increases in most cases. The k dependence of the scissors operator is estimated to about 0.1 eV for Si.[13] Such a variation is certainly negligible for static properties, although may play a minor role in obtaining quantitative agreement near the band edge, i.e., for photon energies above (say) 3 eV.

Next, consider the *sensitivity to the number of k points* included in our Brillouin-zone quadratures. As detailed in Table VII, the strains lower the symmetry of the crystal, and hence increase the size of the irreducible Brillouin zone. We obtain agreement to no worse than 1 microhartree, and possibly much better, in eigenvalues when the different symmetries are used (i.e., when we allow "accidental degeneracies") in the calculation of the

TABLE VII. Special-**k**-point sets for various symmetries. Each column represents an identical set of **k** points for the unstressed crystal. $N_{\rm sym}$ refers to the number of useful point-group operations; as our program includes time-reversal symmetry automatically, we present the number of group elements used explicitly by our program: This will be half the number of elements in the point group if T is a subgroup of the point group. All indicated group operations are symmorphic. $N_{\rm atom}$ refers to the number of atoms in the unit cell, for the cells we have chosen. In the first three lines, N_{kpt} refers to the number of integration points in the irreducible Brillouin zone. In the final two lines, N_{kpt} represents the linear and volume densities of integration points in the Brillouin zone, respectively.

Condition	Point group	$N_{\rm sym}$	$N_{\rm atom}$	N_{kpt}	
Undistorted	$(O_h\otimes T)/T$	24	2	28	60
[001] strain	$(D_{2d}\otimes T)/T$	8	4	36	80
[111] strain	$(C_{3v}\otimes T)/T$	6	2	91	204
Linear density	$2\pi/a$			6	8
Volume density	$(2\pi/a)^3$			216	512

TABLE VIII. The effect of N_{kpt}, the number of integration points in the irreducible Brillouin zone, on the dielectric function and photoelastic tensor at three photon energies. The lattice constants are given in the caption of Table IV. As noted in Table VII, the quadratures using 28, 36, and 91 integration points in the irreducible Brillouin zone—the *odd* lines in the table—represent equivalent integrations in the full Brillouin zone. Similarly, the quadratures using 60, 80, and 204 integration points—the *even* lines in the table—are also equivalent. The sensitivity to the N_{kpt} is not expected to vary strongly with the lattice constant.

			Photon energy (eV)		
		N_{kpt}	0	2.75	3.25
ϵ	a_{LDA}	28	10.95	16.47	22.15
		60	10.88	16.26	21.66
$p_{11}+2p_{12}$	a_{LDA}	28	−0.046	−0.180	−0.337
		60	−0.041	−0.165	−0.279
$p_{11}-p_{12}$	a_{LDA}	36	−0.113	−0.083	−0.028
		80	−0.119	−0.098	−0.067
p_{44}	a_{expt}	91	−0.047	−0.046	−0.041
		204	−0.050	−0.051	−0.051

unstrained crystal. Table VIII illustrates the effect of increasing the density of integration points in the full Brillouin zone by a factor of about 2.4, i.e., going from what is usually known as "28 special points"[23] to "60 special points." In the static limit, values change by 1–10%; at higher frequencies the quantities become more sensitive to the number of special points. In particular, the variation in $p_{11}-p_{12}$ at 3.25 eV is so large as to render this value unreliable (and it is not reported in Fig. 2). We expect a greater variation in all integrated quantities for photon energies approaching the direct band gap. For this photon energy and above, the integrand becomes singular, and therefore is either slowly convergent or requires sophisticated integration methods.

We did not test the sensitivity of the predictions of this study to the energy cutoff in our plane-wave basis. However, earlier work by our group[9] indicated that ϵ is converged to a few parts in 10^3 in the case of GaAs for a 10-hartree cutoff. The convergence in silicon is expected to be somewhat more forgiving, leading to a relative uncertainty of perhaps 10^{-3}, or 0.01 in absolute numbers. We regarded this value as small enough not to warrant a detailed test.

Overall, we believe the static values we present are accurate within the model to a few percent, and those at photon energies of up to 2.75 eV are accurate to 20%.

B. Thermal effects and particle-hole interactions

To address the discrepancies between our predictions and the measured dispersion of $p_{11}-p_{12}$ and p_{44} from about 1.5–2.75 eV, we consider thermal effects and particle-hole interactions.

Although the photoelastic-tensor coefficients have only been measured at room temperature, temperature dependence of $\epsilon(\omega)$ is available.[24,25] We plot in Fig. 5 the dielectric function below the gap in a particular combination that is known to give a straight line throughout nearly the entire subband-gap regime.[26] (The function is well described by a single-oscillator model, as discussed in subsection C.) In Fig. 6 an expanded view is given of the region in which values are known at several temperatures. Extrapolating the two experimental curves to zero temperature will give a value nearly coincident with our $\Delta=0.7$ eV curve both in the static limit (where both experiment at 0 K and $\Delta=0.7$ eV lead to $\epsilon=11.4$) and the slope. A value of Δ near 0.6 eV would be coincident with the 300-K line. Hence, the thermal shift from 0 to 300 K is roughly equivalent to subtracting 0.1 eV from the band gap. Such an observation is consistent with experimental observation of a shift of −50 meV in the direct band gap as the temperature is raised from 4 to 190 K, as presented in Table VI.

An estimate of the effect of a −0.1-eV shift in the band gap may be obtained using the data in Table V. For $p_{12}-p_{11}$, a reduction of about 0.007 is expected at 2.75 eV photon energy, which is much smaller than the 0.03–0.05 reduction required to obtain agreement with

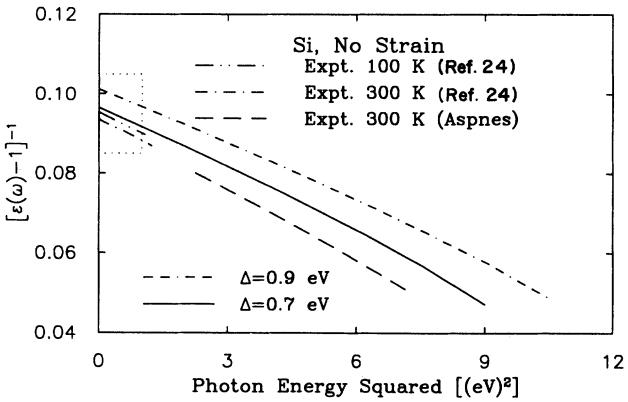

FIG. 5. Dielectric function of unstrained silicon in the combination $[\epsilon(\omega)-1]^{-1}$ as a function of the square of photon energy, for $0\le\omega^2\le10$ eV^2. Such a plot is usually nearly linear for semiconductors below their direct band gaps (Ref. 26), which occurs for $\omega^2\approx11.6$ eV^2 in silicon. Experimental values are given for 100 K (Ref. 24) and 300 K (Refs. 24 and 25). The box bounded by the three dotted lines and the ordinate is expanded in Fig. 6.

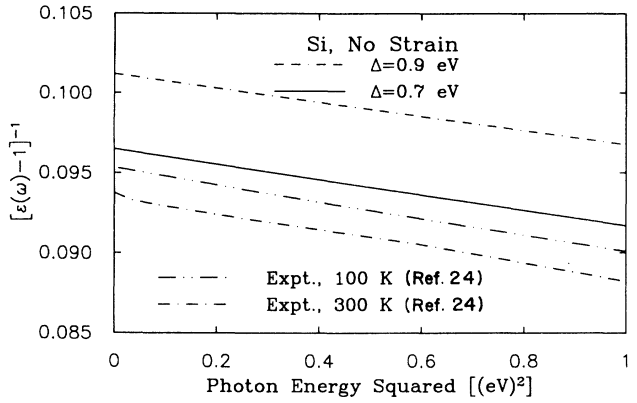

FIG. 6. Dielectric function of unstrained silicon in the combination $[\epsilon(\omega)-1]^{-1}$ as a function of the square of photon energy for $0\leq\omega\leq 1$ eV. These data are an expanded region of the plot in Fig. 5. Experimental values presented at 100 and 300 K are those suggested by Li (Ref. 24). The shift due to temperature change is seen to be roughly equivalent to a shift due to a change in Δ.

experiment. For p_{44}, there is almost no Δ dependence, so this mechanism is completely unimportant. For ϵ, our $\Delta=0.9$ eV value of 10.9 differs by 0.8 from the 300-K value of 11.7, but only 0.5 from the 0-K value of 11.4.

Band theory neglects electron-hole interactions. The *GW* approximation determines improved values for the one-electron Green's function; electron-hole interactions are outside its scope. As a by-product of an attempt to understand the optical-absorption spectrum of silicon, Hanke and Sham[27] calculated the effect of the electron-hole interaction on the static dielectric constant; they predict a shift of +0.55 (from 9.85 to 10.4) for ϵ due to this interaction. Their calculation is performed with a model band structure, so the exact value presented here is not to be taken too seriously. (The Hanke-Sham[27] value of 8.0 for the static dielectric constant in the LDA compares to 13.2 in the present work, and 12.7 and 13.0 in other high-quality calculations.[28,29]) An additional shift of +0.5 in ϵ is just what is required to bring the $\Delta=0.9$ eV calculation of ϵ into agreement with the 0-K value of 11.4. In terms of a variation in Δ, we crudely model the shift due to particle-hole interactions by deducting 0.2 eV from the self-energy correction. Such a shift would translate into a reduction of about 0.015 in $p_{12}-p_{11}$ at $\omega=2.75$ eV, which, in combination with the 0.007 thermal shift, is nearly sufficient to obtain marginal agreement with the data. Of course, the static limit would move away from the data of Higginbotham *et al.*[2] by about 3% (but towards the data of Biegelsen[1]) and away from the data of Grimsditch *et al.*[4] just above the indirect band gap. Hence, it is not likely that particle-hole effects will lead to a match of the measured[4] dispersion of $p_{11}-p_{12}$ above the indirect band gap. There is no effect on p_{44}, since Δ has very little effect on it, at least for $\zeta=0.53$.

The detailed quantitative argument in the above paragraphs is not to be taken literally. The main point is that thermal effects and particle-hole–interaction effects are of the correct order of magnitude to remedy some, but not all, discrepancies with experiment. They are of the same order of magnitude as each other, and their sign is the same. An improved theory should take both effects into account.

C. Single-oscillator model

In this subsection we compare our calculation and experimental data to the simple "single-oscillator model." Wemple and DiDomenico[26] observed that the dielectric function of a large number of semiconductors obeys

$$\epsilon(\omega)=1+\frac{f}{\omega_0^2-\omega^2}\ , \tag{15}$$

for some oscillator strength f and oscillator frequency ω_0. Such a relationship suggests that a plot of $[\epsilon(\omega)-1]^{-1}$ against ω^2 will lie on a straight line. This is verified for both theory and experiment in Figs. 5 and 6.

We wish to extend this model to the case of strain-induced birefringence. The simplest model is to imagine that under some strain μ_{kl} the dielectric tensor is given by

$$\epsilon_{ij}(\omega)=\delta_{ij}+\frac{\delta_{ij}f+f_{ijkl}\mu_{kl}}{(\omega_0+\omega_{0kl}\mu_{kl})^2-\omega^2} \tag{16}$$

to first order in the strain. Expanding to first order in the strain and neglecting terms of order $(\omega/\omega_0)^4$, which is consistent with the single-oscillator assumption,[26] we arrive at

$$\epsilon_{ij}(\omega)=\delta_{ij}+\frac{\delta_{ij}f+f_{ijkl}\mu_{kl}-2\delta_{ij}f\omega_0\omega_{0kl}\mu_{kl}}{\omega_0^2-\omega^2}\ . \tag{17}$$

The constants are not important in this connection—only the ω dependence. For two directions of polarization with components $\hat{e}_i^{(1)}$ and $\hat{e}_i^{(2)}$,

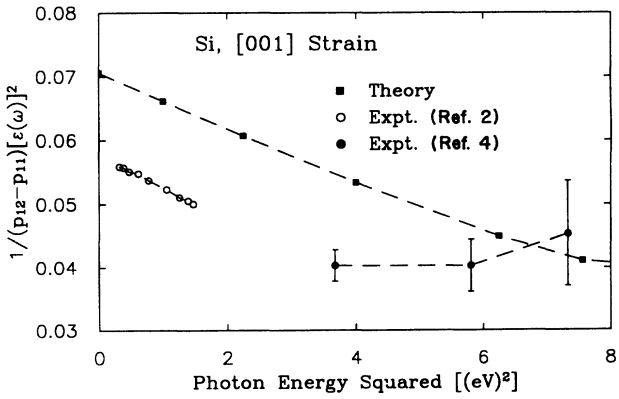

FIG. 7. Photoelastic coefficient and dielectric function plotted in the combination $1/\{(p_{12}-p_{11})[\epsilon(\omega)]^2\}$, as suggested by the single-oscillator model. The single-oscillator model suggests that these data should fall on a straight line. This condition obtains for the calculation and the data of Higginbotham *et al.* (Ref. 2), but not for those of Grimsditch *et al.* (Ref. 4).

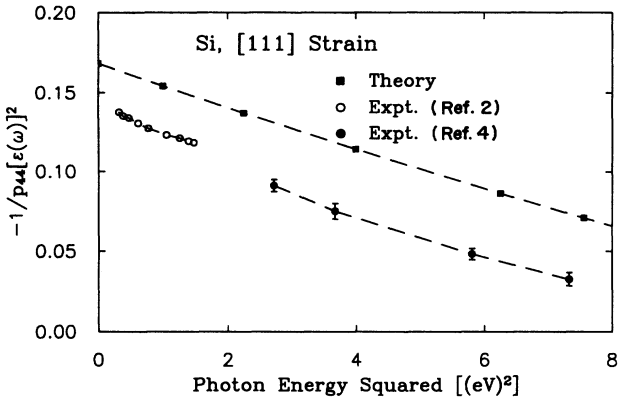

FIG. 8. Photoelastic coefficient and dielectric function plotted in the combination $-1/\{p_{44}[\epsilon(\omega)]^2\}$ as suggested by the single-oscillator model. The single-oscillator model suggests that these data should fall on a straight line. The low-frequency data of Higginbotham *et al.* (Ref. 2) and the higher-frequency data of Grimsditch *et al.* (Ref. 4) are in marginal agreement with a single-oscillator model.

$$\hat{e}_i^{(1)}\hat{e}_j^{(1)}\epsilon_{ij}(\omega)-\hat{e}_i^{(2)}\hat{e}_j^{(2)}\epsilon_{ij}(\omega) = \frac{(\hat{e}_i^{(1)}\hat{e}_j^{(1)}-\hat{e}_i^{(2)}\hat{e}_j^{(2)})f_{ijkl}\mu_{kl}}{\omega_0^2-\omega^2} . \quad (18)$$

By the definition of the photoelastic tensor in Eq. (2), the combination $p\epsilon(\omega)^2$ is proportional to the left-hand side of Eq. (18): The single-oscillator model predicts a linear plot of $1/\{p[\epsilon(\omega)]^2\}$ against ω^2.

We show such plots for the [001] strain in Fig. 7 and for [111] strain in Fig. 8. The single-oscillator model is obeyed by the theory in both plots. For the [001] strain, the low-frequency measurements[2] are in accord with the single-oscillator model, but for the values above the indirect band gap the data[4] obey a substantial deviation. For the [111] direction the low- and high-frequency measurements show a marginal disagreement with the single-oscillator model, primarily in the form of a misalignment of the low- and high-frequency data. A decrease in the high-frequency value of p_{44} would improve the agreement with the single-oscillator model, as well as agreement with our calculation. Noise in the slope of the low-frequency data for the [111] direction make it a less reliable predictor of the high-frequency regime than for the [001] case. The indirect band gap plays no role in our theory, but the absorptions considerably complicate the measurements. The failure of the data, particularly for [001] strain, to obey the single-oscillator model suggests that these data may not be valid.

Wemple and DiDomenico have considered an alternate extension, leading to the conclusion that a plot of $p/(1-1/\epsilon)^2$ against ω^2 will lie on a straight line.[30] We do not present these plots; however, their analysis leads to substantially the same conclusion: a well-defined inconsistency for the low- and high-frequency measurements of $p_{11}-p_{12}$ and an ambiguous result for the p_{44}. Our calculated values obey the single-oscillator model (i.e., fall on a straight line) for this plot as well.

IV. CONCLUSIONS

We have calculated all independent components of the photoelastic tensor of silicon using the Kohn-Sham local-density approximation (LDA) with a self-energy correction in the form of a "scissors operator," as well as the ordinary dielectric function. This work is an extension of previous successful calculations of the dielectric function and nonlinear susceptibility for second-harmonic generation of semiconductors.

We achieve good agreement with all components for low frequencies. It is necessary to use the experimental lattice constant (rather than that predicted by minimizing the LDA total energy) to achieve this agreement in the case of the components associated with hydrostatic compression.

We omit thermal effects and electron-hole interactions in the calculation. While we estimate that these effects are probably sufficient to bring the calculated dielectric function into agreement with experiment, the agreement for the piezobirefringence coefficients may be improved only to a limited extent. Consideration of a single-oscillator model indicates that the measured values below and above the indirect band gap may not be consistent with each other, particularly for strains applied in the [001] direction.

ACKNOWLEDGMENTS

This work was supported by the Division of Materials Research of the Office of Basic Energy Science of the U.S. Department of Energy, and by the Cornell National Supercomputer Facility (at Cornell University, Ithaca, NY).

*Present address: School of Physics, Georgia Institute of Technology, Atlanta, GA 30332.

[1]D. K. Biegelsen, Phys. Rev. Lett. **32**, 1196 (1974); Phys. Rev. B **12**, 2427 (1975).
[2]C. W. Higginbotham, M. Cardona, and F. H. Pollak, Phys. Rev. **184**, 821 (1969).
[3]M. Chandrasekhar, M. H. Grimsditch, and M. Cardona, Phys. Rev. B **18**, 4301 (1978).
[4]M. H. Grimsditch, E. Kisela, and M. Cardona, Phys. Status Solidi A **60**, 135 (1980).
[5]Z. H. Levine and D. C. Allan, Phys. Rev. B **43**, 4187 (1991).
[6]M. P. Surh, S. G. Louie, and M. L. Cohen, Phys. Rev. B (to be published).
[7]Z. H. Levine and D. C. Allan, Phys. Rev. Lett. **63**, 1719 (1989).
[8]Z. H. Levine and D. C. Allan, Phys. Rev. Lett. **66**, 41 (1991).
[9]Z. H. Levine and D. C. Allan, Phys. Rev. B **44**, 12 781 (1991).
[10]M. P. Teter, M. C. Payne, and D. C. Allan, Phys. Rev. B **40**, 12 255 (1989).
[11]L. Hedin, Phys. Rev. **139**, A796 (1965); L. Hedin and S. Lundqvist, in *Solid State Physics*, edited by H. Ehrenreich, F.

Seitz, and D. Turnbull (Academic, New York, 1969), Vol. 23, p. 1.
[12]M. S. Hybertsen and S. G. Louie, Phys. Rev. B **34**, 5390 (1986).
[13]R. W. Godby, M. Schlüter, and L. J. Sham, Phys. Rev. B **37** 10 159 (1988).
[14]X. Zhu, S. Fahy, and S. G. Louie, Phys. Rev. B **39**, 7840 (1989); **40**, 5821(E) (1989).
[15]S. L. Adler, Phys. Rev. **126**, 413 (1962).
[16]N. Wiser, Phys. Rev. **129**, 62 (1963).
[17]M. Born and E. Wolf, *Principles of Optics* (Permagon, New York, 1975), p. 679.
[18]J. F. Nye, *Physical Properties of Crystals,* 2nd ed. (Oxford University Press, New York, 1985), Chaps. 8 and 13.
[19]L. Kleinman, Phys. Rev. **128**, 2614 (1962).
[20]A. Segmüller and H. R. Neyer, Phys. Kondens. Mater. **4**, 63 (1965).
[21]O. H. Nielsen and R. M. Martin, Phys. Rev. B **32**, 3792 (1985).
[22]S. Wei, J. W. Wilkins, and D. C. Allan (unpublished). This paper gives additional references regarding the internal relaxation parameter ζ.
[23]H. J. Monkhorst and J. D. Pack, Phys. Rev. B **13**, 5188 (1976).
[24]H. H. Li, J. Chem. Phys. Ref. Data **9**, 561 (1980).
[25]D. E. Aspnes and A. A. Studna, Phys. Rev. B **27**, 985 (1983).
[26]S. H. Wemple and M. DiDomenico, Jr., Phys. Rev. Lett. **23**, 1156 (1969); Phys. Rev. B **3**, 1338 (1971).
[27]W. Hanke and L. J. Sham, Phys. Rev. B **21**, 4656 (1980).
[28]S. Baroni and R. Resta, Phys. Rev. B **33**, 7017 (1986).
[29]M. S. Hybertsen and S. G. Louie, Phys. Rev. B **35**, 5585 (1987).
[30]S. H. Wemple and M. DiDomenico, Jr., Phys. Rev. B **1**, 193 (1970).
[31]D. R. Hamann, Phys. Rev. B **40**, 2980 (1989).
[32]L. Kleinman and D. M. Bylander, Phys. Rev. Lett. **48**, 1425 (1982).
[33]D. M. Ceperley and B. J. Alder, Phys. Rev. Lett. **45**, 566 (1981).
[34]M. P. Teter (unpublished). Teter has provided a parametrization of the electron-gas data of Ceperley and Alder that is differentiable at all electron densities.
[35]M. Welkowsky and A. Braunstein, Phys. Rev. B **5**, 497 (1972).
[36]D. R. Mašović, F. R. Vukajlović, and S. Zeković, J. Phys. C **16**, 6731 (1983).
[37]D. E. Aspnes and A. A. Studna, Solid State Commun. **11**, 1375 (1972).
[38]R. Vetter, Phys. Status Solidi A **8**, 443 (1971).